Journal of Biomolecular NMR, 4 (1994) 689–702
ESCOM

J-Bio NMR 202

Assignment of the protonated ^{13}C resonances of apo-neocarzinostatin by 2D heteronuclear NMR spectroscopy at natural abundance

Claudine Lefevre, Élisabeth Adjadj, Éric Quiniou and Joël Mispelter*

U350 INSERM, Institut Curie Biologie, Centre Universitaire, Bât. 112, F-91405 Orsay Cedex, France

Received 21 January 1994
Accepted 13 April 1994

Keywords: Neocarzinostatin; ^{13}C NMR; Resonance assignments; Secondary chemical shifts; Editing

SUMMARY

Nearly complete assignment of the protonated carbon resonances of apo-neocarzinostatin, a 113-amino acid antitumor antibiotic carrier protein, has been achieved at natural ^{13}C abundance using heteronuclear 2D experiments. Most of the cross peaks in the proton–carbon correlation map were identified by the combined use of HMQC, HMQC-RELAY and HMQC-NOESY spectra, using already published proton chemical shifts. However, double-DEPT and triple-quantum experiments had to be performed for the edition of CH and CH_2 side-chain groups, respectively, which were hardly visible on HMQC-type maps. The triple-quantum pulse sequence was adapted from its original scheme to be applicable to a natural abundance sample. The correlation between carbon chemical shifts and the apo-neocarzinostatin structure is discussed. In particular, ^{13}C alpha secondary shifts correlate well with the backbone conformation. These shifts also yield information about the main-chain flexibility of the protein. Assignments reported herein will be used further for interpretation of carbon relaxation times in a study of the internal dynamics of apo-neocarzinostatin.

INTRODUCTION

^{13}C and ^{15}N NMR spectroscopy have long been recognized as powerful tools for studying structural and dynamic properties of biological molecules (Wüthrich, 1976). However, earlier investigations were dramatically limited, both in resolution and in sensitivity, due to the low natural abundance and weak gyromagnetic ratio of the heteronuclei and because 1D experiments were recorded with direct ^{13}C or ^{15}N observation (Oldfield et al., 1975; Norton et al., 1977; London and Avitabile, 1978; Ribeiro et al., 1980; Richarz et al., 1980). Introduction of 2D heteronuclear reverse spectroscopy at high fields (Ernst et al., 1987; Wagner et al., 1989) and the availability of isotopically enriched samples greatly circumvented these problems. Heteronuclear correlated experiments are now increasingly used to assign proton spectra of large proteins

*To whom correspondence should be addressed.

and/or to give an insight into their internal motions. However, most of the current papers concentrate on ^{15}N resonance assignments and the database containing ^{13}C chemical shifts remains limited. Recently, several studies have given evidence for a clear correlation between the chemical shifts of $^{13}C^{\alpha}$ and $^{13}C^{\beta}$ carbons and the protein backbone conformation (Spera and Bax, 1991; Wishart et al., 1991). The contribution of hydrogen bonding and charge-field effects was found to be small compared to that of the ϕ,ψ torsion angles. Ab initio computations of nuclear shielding led to similar conclusions (de Dios et al., 1993; Laws et al., 1993).

We report here the nearly complete assignment of the protonated ^{13}C resonances of apo-neocarzinostatin, a 113-amino acid protein. Its three-dimensional structure has already been elucidated by homonuclear ^{1}H NMR (Adjadj et al., 1990,1992a; Remerowski et al., 1990; Gao and Burkhart, 1991; Gao, 1992) and by X-ray crystallography (Teplyakov et al., 1993). More recently, a crystal structure of the holo-protein has been reported at 0.18 nm resolution (Kim et al., 1993). In its native form, apo-neocarzinostatin binds a chromophore with antitumour antibiotic properties. The apo-protein is essential for the stability and transport of its chromophore (Kappen et al., 1980). The flexibility of the loops involved in the binding site, as suggested from rms deviations between NMR structures (Adjadj et al., 1992a,b) and from B-factors of X-ray data (Teplyakov et al., 1993), is thought to play a role in the biological activity of this carrier protein. In order to obtain further knowledge of main-chain internal motions, relaxation parameters of protonated ^{13}C nuclei have to be measured. The first step is an assignment of the ^{13}C spectrum for apo-neocarzinostatin. Since no isotope enrichment was used, the experiments described here may be extended to other proteins of similar weight, provided that about 10 mM samples can be obtained.

The basic pulse sequence used in this study is HMQC (Bax et al., 1983; Bendall et al., 1983). In such an experiment, cross peaks correlate carbon resonances (along $\omega 1$) with the resonances of attached protons (along $\omega 2$) via the one-bond $^{1}J_{CH}$ couplings. The sensitivity would ideally be similar to that of a 2D homonuclear ^{1}H experiment, reduced by a factor of 100 due to the natural abundance of ^{13}C. However, nonperfect elimination of ^{1}H-^{12}C components leads to an increase of the overall noise. As the ^{1}H chemical shifts are known, some resonances can be identified directly in the HMQC spectrum, but their number is limited by strong overlap in the ^{1}H spectrum. However, remote connectivities obtained via homonuclear proton–proton coupling (HMQC-RELAY) (Brühwiler and Wagner, 1986; Lerner and Bax, 1986; Wagner and Brühwiler, 1986) or via ^{1}H-^{1}H NOE effects (HMQC-NOESY) (Oh et al., 1989; Shon and Opella, 1989) help in removing most of the ambiguities. By means of these three experiments, we were able to assign the α-methine carbons and the methyl carbons of apo-neocarzinostatin. In contrast, only a few methylene and side-chain methine resonances could be extracted from the HMQC-type spectra. We then performed double-DEPT-type transfers of magnetization, allowing optimization of $^{13}CH_n$ intensities according to their multiplicity factor n. The sequences used are described extensively in the Materials and Methods section. They are derived from double- (Wagner, 1989) or triple- (Schmidt and Rüterjans, 1990) quantum correlated schemes. Using this strategy, we obtained a nearly complete assignment of the protonated carbons of apo-neocarzinostatin. To our knowledge, this is the first nearly complete assignment for a protein of this size (113 amino acids).

MATERIALS AND METHODS

Apo-neocarzinostatin was purified as described previously (Adjadj et al., 1990). All NMR

experiments were performed at 308 K using a sample containing 9 mM protein in 99.9% D_2O, pH 5.5, at natural ^{13}C abundance. Heteronuclear 2D spectra were recorded on a Varian Unity500 spectrometer, equipped with a broadband triple-resonance probe, optimized for ^1H detection. The data were processed on a Sun Sparc2 workstation, using the available Varian software.

The pulse sequences used for the assignment of ^{13}C resonances are shown in Fig. 1, together with their basic phase cyclings. The ^{13}C frequency scale was indirectly referenced to TMS. The spectral width in $\omega 2$ was 6000 Hz, with the carrier set to the HDO resonance frequency. Depending on specific experiments, the spectral width in $\omega 1$ was taken between 6000 and 8000 Hz. During acquisition, decoupling of ^{13}C spins was performed on a relatively small spectral band to limit sample heating. A ^1H reference spectrum was run before and after each experiment, to check that no degradation of the sample had occurred during the long measurement times (between 22 and 56 h). Band-pass or high-pass filters were inserted in the lock, proton and carbon lines to eliminate possible interferences between the rf channels.

Numerous sequences have been proposed to obtain 2D one-bond correlated spectra: double DEPT or double refocused INEPT (Wagner, 1989), Müller's sequence (Müller, 1979), HMQC (Bax et al., 1983; Bendall et al., 1983), HSQC (Bodenhausen and Ruben, 1980) and derivatives of the last two sequences (Bax et al., 1990; Zuiderweg, 1990; Palmer et al., 1991), designed to enhance the sensitivity and/or resolution. We performed the HMQC experiment for its simplicity and short measuring time. However, ^{13}C-^1H multiple-quantum correlation techniques (unlike single-quantum ones) suffer from unresolved homonuclear J_{HH} couplings in the $\omega 1$ dimension that alter the available resolution (Bax et al., 1990; Norwood et al., 1990; Zuiderweg, 1990). The key point is then to choose sufficiently short t_1 acquisition times ($\ll 1/J_{HH}$), so that the line shapes will not be seriously affected (Summers et al., 1986). The HMQC spectrum was used as a starting point in the assignment procedure. A great number of uncertainties were removed using relayed connectivities, obtained in the HMQC-RELAY spectrum. As can be seen in Fig. 1, the related sequence consists of an HMQC scheme, followed by a transfer of magnetization between scalarly coupled protons. The HMQC-NOESY experiment is similar to that described by Shon and Opella (1989). It yields additional information compared to that of HMQC-RELAY (for example, cross-strand connectivities between α-carbon spins and α-proton spins in antiparallel β-sheets, hereafter referred to as $d\alpha\alpha$ connectivities). Few methylene and methine side-chain carbons, with the exception of Ser^β and Thr^β, are visible in HMQC-type spectra. Indeed, they display weak resonances that may be obscured by noise, especially in the ^1H spectral band corresponding to methyl groups. Furthermore, the methylene resonances are broadened and exhibit poorly resolved multiplet structures in the $\omega 1$ and $\omega 2$ dimensions. Other experiments were thus devised in order to (i) obtain higher sensitivity; (ii) reduce the CH_3 signals; and (iii) optimize polarization transfer for CH or CH_2 groups.

Edition of the CH subspectrum was performed by means of a double-DEPT scheme (Fig. 1, sequence c) that has already been used for measurements of ^{13}C relaxation times in proteins (Kay et al., 1987; Sklenar et al., 1987; Nirmala and Wagner, 1988). By setting the flip angle θ in DEPT sequences to 90°, CH_2 and CH_3 signals are dramatically reduced, while CH signals show full intensities (Doddrell et al., 1982). After the first transfer from ^1H to ^{13}C, carbon magnetization is stored along the z-axis. A ^1H purge pulse, followed by a z gradient pulse, is then used to eliminate the ^1H and ^1H-^{12}C resonances (Sklenar et al., 1987; Nirmala and Wagner, 1988). For side-chain methine groups, this resulted in a significant improvement of the overall sensitivity, so that all

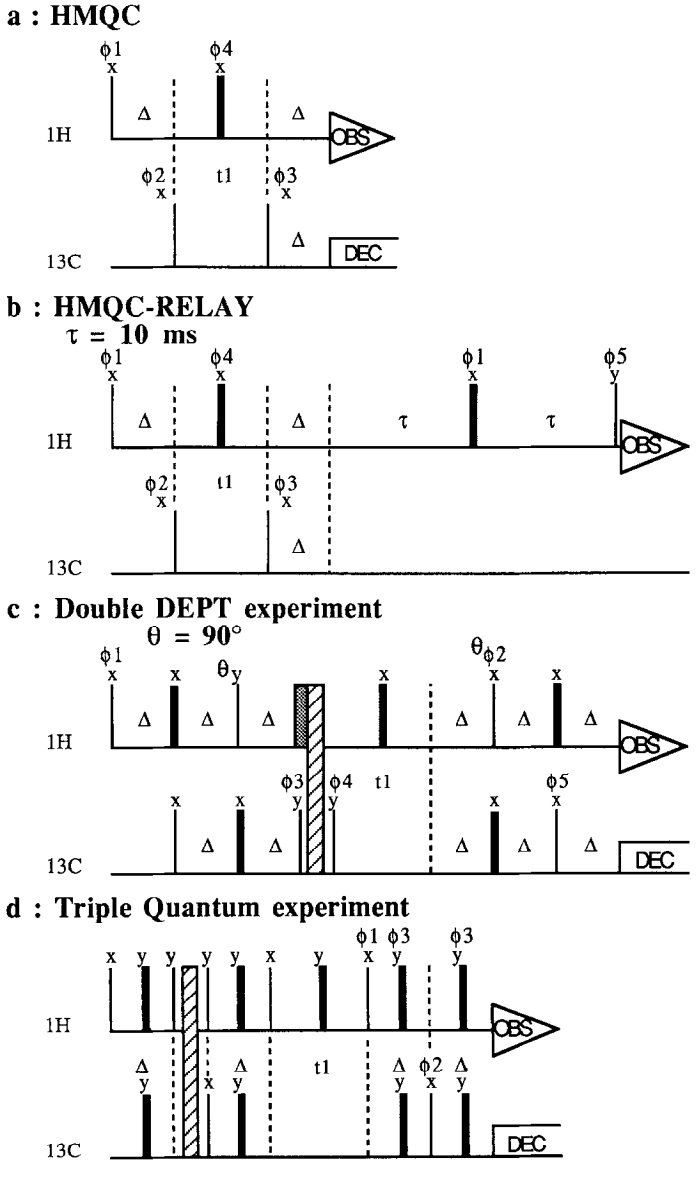

Fig. 1. Pulse sequences for (a) HMQC; (b) HMQC-RELAY; (c) double-DEPT; and (d) triple-quantum experiments. Thin and thick vertical bars represent 90° and 180° pulses, respectively. The flip angles θ in sequence c are set equal to 90°. The dotted bar represents a 3 ms purge pulse, and hatched bars represent 0.5 ms homogeneity spoiling z gradient pulses. After each z gradient pulse, a 3 ms delay is applied for recovery of magnetic field homogeneity. The delay Δ is set to 3.3 ms, which is slightly less than the mean $1/2J_{CH}$, in order to minimize relaxation losses. Quadrature detection in the ω1 dimension was performed by incrementing the phase of the 90° ^{13}C pulse that precedes the t_1 evolution period. WALTZ-16 decoupling (Shaka et al., 1983) of carbon resonances during detection was used, except in the HMQC-RELAY experiment. In (a) and (b), the basic phase cycling is: ϕ1 = ϕ3 = ϕ4 = (x,x,y,y); ϕ2 = (x,−x,y,−y); ϕ5 = (y,y,−x,−x); Rec = (x,−x,y,−y). In addition, phase ϕ4 of the 180° ^1H refocusing pulse in the middle of the evolution period is incremented by 90° every four scans and phase ϕ3 of the last 90° ^{13}C pulse is inverted every 16 scans (together with inversion of the receptor phase). In (c), the basic phase cycling is: ϕ1 = (x,−x); ϕ2 = (x,x,−x,−x); ϕ3 = (y,−y); ϕ4 = 4y,4(−y); ϕ5 = (x,x,−x,−x); Rec = 4x,4(−x). In (d), it is: ϕ1 = (x,−x); ϕ2 = (x,x,−x,−x); ϕ3 = (y,−y); Rec = (y,−y,−y,y). A CYCLOPS is added in schemes c and d.

resonances could be assigned unambiguously. The pulse sequence c also allowed identification of several aromatic resonances.

Methylene carbon editing was performed using a triple-quantum experiment. The related pulse sequence (Fig. 1, sequence d) is derived from that of Schmidt and Rüterjans (1990) and allows the exclusive detection of I_2S spin systems (with I = ^{1}H and S = ^{13}C). It is based on a double polarization transfer by means of modified DEPT schemes, implying the formation of triple-quantum coherences ($I_x^1 I_y^2 S_x$-like terms in the notation of the product operator formalism (Sørensen et al., 1983)) during t_1. Delays for refocusing of the heteronuclear one-bond couplings (the last delay Δ in DEPT and the first delay Δ in RDEPT, respectively) are omitted in the polarization transfers. The resulting time saving is expected to limit signal loss due to transverse relaxation. The original triple-quantum pulse sequence was modified to suppress the intense ^{1}H-^{12}C resonances prior to detection. Bringing the magnetizations of interest along the z-axis as heteronuclear longitudinal spin order I_zS_z, while the others remain in the transverse plane, and destroying the unwanted ^{1}H-^{12}C signals by application of a z gradient has been shown to be particularly efficient in heteronuclear COSY and RELAY experiments (Brühwiler and Wagner, 1986). This procedure has also been reported in an E-HMQC experiment (Zhang and Wang, 1991). However, simultaneous ^{1}H and ^{13}C 180° pulses have to be added in the two polarization transfers, in order to remove chemical shift contributions. The final sequence has the advantage over earlier 2D heteronuclear correlation schemes with inverse ^{1}H editing (Sklenar et al., 1987; Kay and Bax, 1989; Kessler et al., 1989; Davis, 1990,1991; Domke and Leibfritz, 1990; Tate et al., 1991; Zhang and Wang, 1991) that it is applicable to ^{13}C natural abundance samples and allows exclusive detection of I_2S spin systems in a single 2D spectrum. The triple-quantum experiment was successfully performed on apo-neocarzinostatin and was very helpful in the assignment of CH_2 resonances.

RESULTS

Carbon assignment strategy

Given the knowledge of all the ^{1}H chemical shifts of apo-neocarzinostatin (Adjadj et al., 1990), and the fact that ^{13}C chemical shifts are located in characteristic regions of the spectrum, depending on the carbon and residue types (Wüthrich, 1976; Howarth and Lilley, 1978), half of the resonances could be directly assigned in the HMQC spectrum. Cross peaks with similar ^{1}H positions ($\Delta\delta \leq 0.02$ ppm) were assigned from the HMQC-RELAY (Fig. 2) and HMQC-NOESY spectra. The double-DEPT and triple-quantum experiments were used for the edition of methine and methylene groups, respectively.

Methine α-carbon assignments

Out of the 98 methine α-carbons, 76 were assigned unambiguously in the HMQC spectrum using the known ^{1}H chemical shifts and allowing the actual ^{13}C shifts to differ from standard values (Wüthrich, 1976) by ± 4 ppm (occasionally more, when no peak was present in the search region). The resonances of Ala^{59} and Ala^{100} were found to be completely degenerate both in ^{1}H and ^{13}C chemical shifts. Not surprisingly, Ala^1 exhibits a characteristic narrow quadruplet fine structure – it is expected to be very mobile. The remaining 22 methine α-carbon resonances, that could not be assigned directly, are either resonances with overlapping ^{1}H chemical shifts, resonances which fall out of their expected area, or resonances which are not visible. A combined

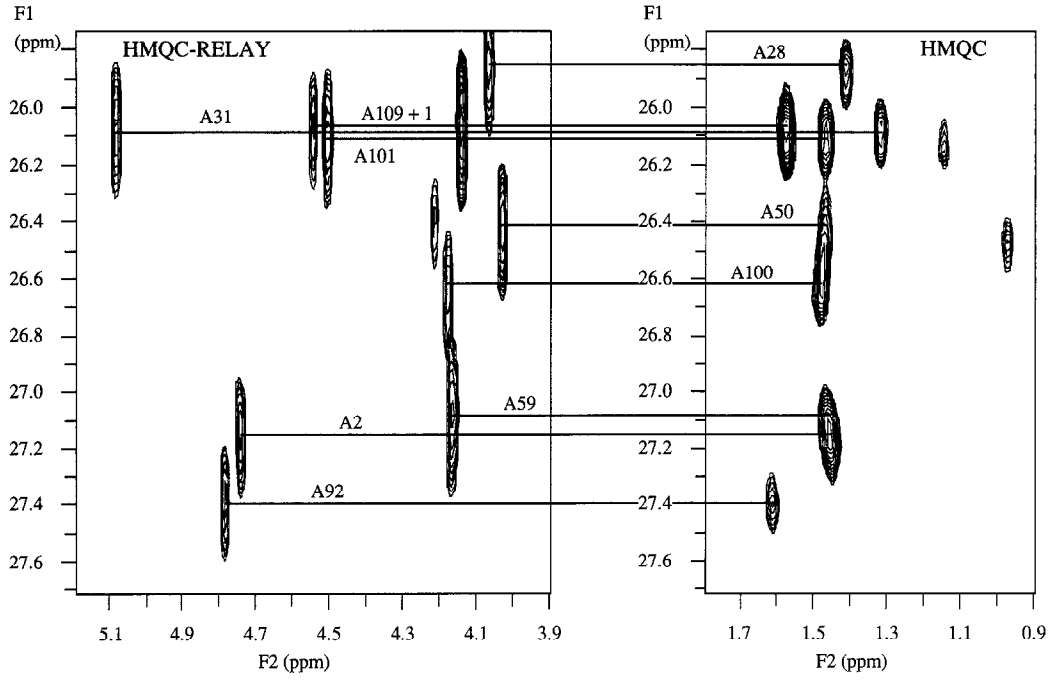

Fig. 2. Example of the combined use of the HMQC and HMQC-RELAY experiments in the assignment procedure. Heteronuclear correlation spectra for some alanine spin systems are shown. Direct methyl beta connectivities (in the HMQC spectrum) and remote connectivities to the alpha proton (in the HMQC-RELAY spectrum) appear on the same horizontal line. The RELAY experiment was recorded with pulse sequence b of Fig. 1, with $\tau = 10$ ms.

study of the HMQC-RELAY and HMQC-NOESY spectra allowed us to solve most of the uncertainties. All but two residues with overlapping ^{1}H chemical shifts (Arg^{71} and Cys^{88}) were thus assigned on the basis of remote connectivities in the HMQC-RELAY or HMQC-NOESY spectra, and by exclusion. The α-carbon resonance of Arg^{70} is found to be shifted upfield by 5.1 ppm from its random coil value, probably due to a disruption in the secondary structure: the polypeptide chain turns in this position by about 90° (Adjadj et al., 1992a). Asp$^{87\alpha}$ was assigned on the basis of a dαα-type connectivity with Ser$^{72\alpha}$ in the HMQC-NOESY spectrum. Asp$^{99\alpha}$ was identified at the end of the assignment procedure. Unassigned α-resonances are those of Arg^{71}, Cys^{88} and Pro^{49}, for which no relayed information was obtained. While the last two resonances are not visible in the HMQC spectrum – unless they are hidden below an already identified connectivity – two peaks appear at similar ^{1}H positions to that of Arg^{71} (around 2.26 ppm, because of a strong ring-current effect), and respectively at 56.35 and 61.35 ppm in the ^{13}C dimension. These could not be assigned, neither on the basis of their ^{13}C chemical shifts nor on the basis of their ^{1}H fine structure.

Methyl carbon assignments

Methyl groups show the most intense peaks in the upfield aliphatic region of the spectrum. Because of the small ^{13}C spectral width (6700 Hz) chosen for the HMQC experiment, many of them are folded in the carbon dimension, so they appear among methylene resonances. However, no confusion is possible, due to their great intensities and narrow lineshapes compared to the

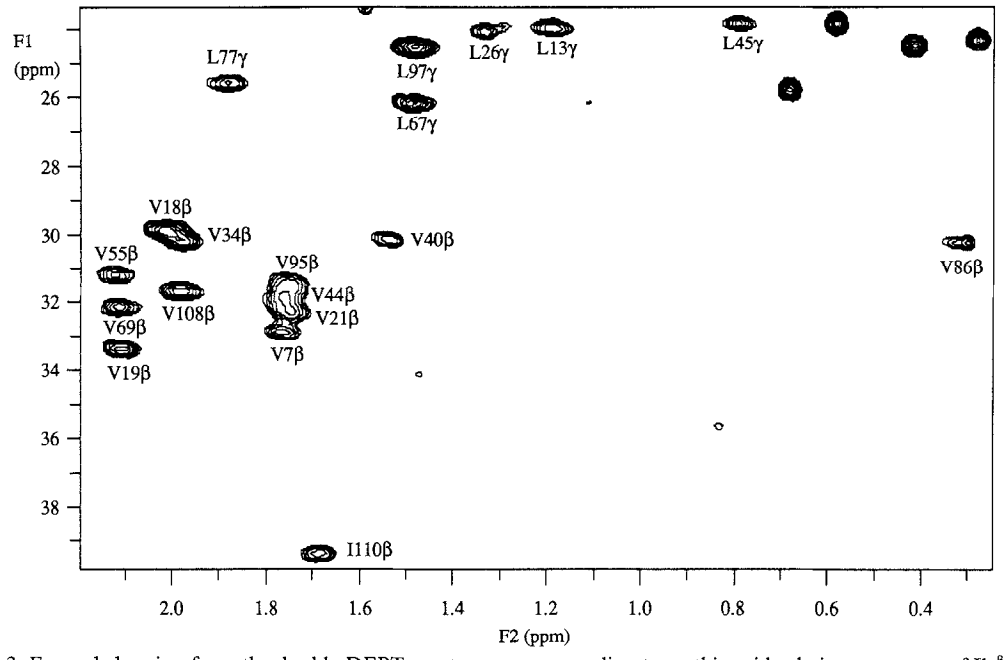

Fig. 3. Expanded region from the double-DEPT spectrum, corresponding to methine side-chain resonances of Ile^{β}, Val^{β} and Leu^{γ}. The four intense cross peaks that appear at the top right edge belong to CH_3 groups. 128 increments in t_1 were collected, with 2 FIDs per increment for quadrature detection in the ω1 dimension and 128 scans per FID. The total measurement time was approximately 22 h. 85°-shifted sine-bell filtering was used in t_1, and 70°-shifted squared sine-bell filtering in t_2.

broad and weak CH_2 resonances. Only 39 methyl peaks out of 69 were assigned directly in the HMQC spectrum, because of extensive ^1H spectral overlap. The HMQC-RELAY experiment proved to be particularly useful, yielding for instance almost all the relayed Ala^{α} connectivities, as can be seen in Fig. 2. In fact, 64 out of the 69 methyl resonances could be identified unambiguously. Nonassigned resonances are $Val^{21\gamma1}$, $Val^{34\gamma1\gamma2}$, $Val^{95\gamma1}$ and $Val^{108\gamma1}$, for which no relayed cross peak was observed.

Methine side-chain carbon assignments

Threonine $^{13}C^{\beta}$-$^1H^{\beta}$ cross peaks can be distinguished from other methine side-chain resonances in the HMQC spectrum due to their characteristic $^{13}C^{\beta}$ chemical shifts (66–71 ppm). The 13 threonine β carbons were identified easily by means of the HMQC and HMQC-RELAY experiments. In contrast, Val^{β}, Ile^{β} and Leu^{γ} were hardly visible in HMQC-type spectra, mainly because their ^1H chemical shifts are similar to those of CH_3 groups. A double-DEPT experiment was then found to be particularly useful: it minimized CH_3 signals and revealed unambiguously the 19 side-chain methine resonances of interest (Fig. 3). Note that a larger ^{13}C spectral width was used, in order to avoid methyl folding onto Leu^{γ} cross peaks.

Aromatic ring carbon assignments

Aromatic ring resonances are located downfield, far away from the aliphatic spectrum: between 112 and 132 ppm in the ^{13}C dimension and between 6.8 and 7.6 ppm in the ^1H dimension. In previous HMQC-type spectra, they were extensively folded in ω1. A specific double-DEPT

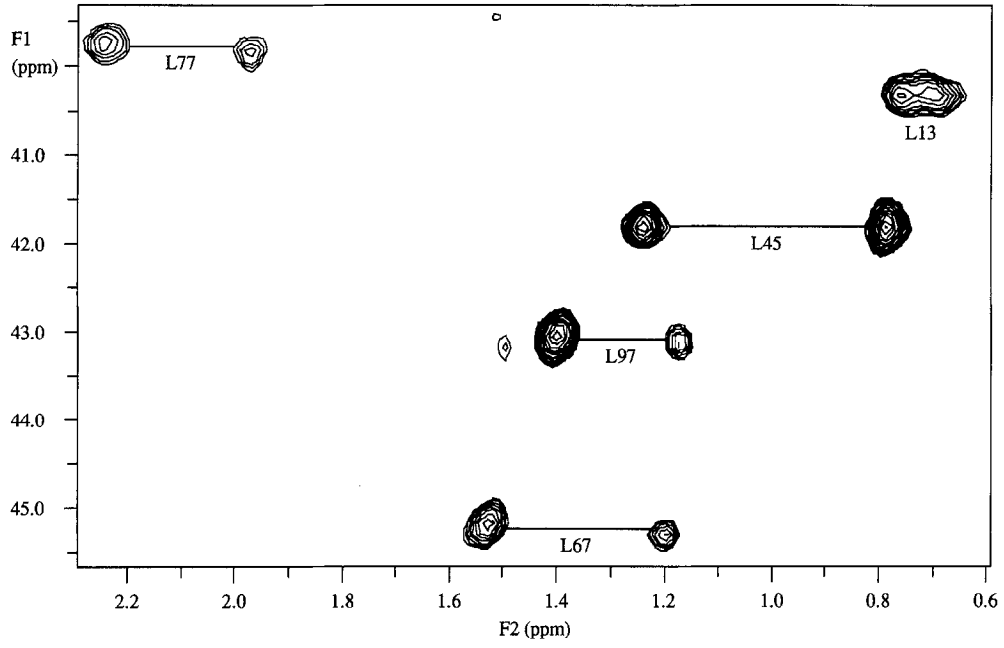

Fig. 4. Part of the triple-quantum spectrum, showing leucine C^{β}-$H^{\beta 1,\beta 2}$ cross peaks. The $Leu^{26\beta}$ resonance is lacking, but the other five resonances appear clearly above the noise level. Proton homonuclear J couplings, which are active during the evolution and detection periods, explain the shift observed between some $^{13}C^{\beta}$-$^{1}H^{\beta 1}$ and $^{13}C^{\beta}$-$^{1}H^{\beta 2}$ cross peaks in the carbon dimension and/or their 45° tilting. 128 increments in t_1 were collected, with 2 FIDs per increment for quadrature detection in the ω1 dimension and 224 scans per FID, resulting in a total acquisition time of 40 h. 85°- and 70°-shifted sine-bell functions were applied in the ω1 and ω2 dimensions, respectively.

experiment, with the ^{13}C carrier at 120 ppm, was performed to allow efficient excitation and detection of protonated aromatic signals. Tryptophan and tyrosine ring resonances (except $Tyr^{32\delta}$) were thus identified, confirming intra-ring remote connectivities already observed in the HMQC-RELAY and HMQC-NOESY spectra. In contrast, phenylalanine resonances suffer from overlap of their ^{1}H and ^{13}C chemical shifts. Only part of them have been assigned, since remote connectivities are hardly interpretable in HMQC-type spectra. $Phe^{112\varepsilon}$ and $Phe^{73\delta}$ are found to be degenerate, both in ^{1}H and ^{13}C positions. We confirm that $Phe^{73\varepsilon}$ and $Phe^{73\zeta}$ have the same proton chemical shift, as was suggested earlier (Adjadj et al., 1990). Phe^{76} and Phe^{78} remain unassigned.

Methylene carbon assignments

One should expect the assignment of methylene carbons to be quite easy, since the cross peaks to both methylene protons must appear at the same carbon chemical shift on the HMQC map. This is only the case for nine resonances out of 92: $Asn^{60\beta}$, $Asn^{113\beta}$, $Phe^{78\beta}$, $Gln^{27\gamma}$, $Glu^{106\gamma}$, $Arg^{71\delta}$, $Arg^{82\delta}$, $Lys^{20\delta}$ and $Lys^{20\varepsilon}$. The others exhibit weak and/or poorly resolved resonances, so that their identification would be unreliable unless additional information is obtained. Ser^{β} cross peaks are packed into a small region (from 3.5 to 4.5 ppm in the ^{1}H dimension, and from 62 to 64 ppm in the ^{13}C dimension). They were assigned by means of relayed connectivities to Ser^{α} in the HMQC-RELAY spectrum. The triple-quantum experiment was used to identify the remaining

resonances. It yielded particularly striking results for Leu^{β} residues, which were previously hidden in the CH_3 noise (see Fig. 4). However, $Leu^{26\beta}$ was still invisible, as were other cross peaks ($Gly^{35\alpha}$, $Gly^{80\alpha}$, $Gly^{104\alpha1}$, $Gln^{36\gamma}$, $Glu^{74\gamma}$, $Arg^{70\beta,\gamma}$, $Arg^{71\gamma}$, $Ile^{110\gamma}$ and all Cys^{β}). Some resonances have been tentatively assigned: $Phe^{52\beta}$ at 40.8–41 ppm (degenerate with $Asp^{51\beta}$), $Asp^{99\beta}$ at 38.65 ppm, $Pro^{49\beta}$ at 28.9 ppm and $Arg^{71\beta}$ at 29.25 ppm. We find that cross peaks have similar aspects in heteronuclear and homonuclear shift-correlated spectra. Thus, residues that could not be identified in this assignment procedure very often display large and weak resonances in the ^1H-^1H COSY spectrum (this is the case for all Cys^{β}).

Table 1 contains all the carbon chemical shifts that have been established as described above. Of the protonated carbon resonances of apo-neocarzinostatin, 90% were assigned.

DISCUSSION

It has been shown that for unstructured peptides, the carbon chemical shifts of one amino acid do not depend on the chemical nature of its neighbours, except when the following residue is a proline (Howarth and Lilley, 1978). In a protein, deviations from random coil chemical shifts, often referred to as secondary shifts, are thus determined by the secondary or tertiary structure, but not by the amino acid sequence. Only the residues preceding proline do not follow this rule, having in particular $^{13}C^{\alpha}$ resonances shifted upfield from random coil values (Clore et al., 1990). Apo-neocarzinostatin contains four prolines, at positions 3, 9, 49 and 105. The $^{13}C^{\alpha}$ of Ala^2, Thr^8 and Asp^{48} indeed exhibit this upfield shift. In contrast, for Gly^{104} this trend is not valid. The flexibility of the loop region where Gly^{104} is located could affect its observed chemical shift. Cis-trans isomerism of proline may also be deduced from C^{β} and C^{γ} chemical shifts. Pro^9 has already been shown to be in a cis conformation (Remerowski et al., 1990; Teplyakov et al., 1993), while the other three proline residues are in a trans conformation. Characteristic remote connectivities in the HMQC-NOESY spectrum confirm this fact: if X represents the residue preceding proline, then NOEs between X^{α} and Pro^{δ} are observed in case of a proline trans conformation, whereas NOEs between X^{α} and Pro^{α} are observed in case of a proline cis conformation (this was verified for Ala^2-Pro^3, Thr^8-Pro^9 and Asp^{48}-Pro^{49}). Moreover, C^{β} and C^{γ} resonances of Pro^9 are shifted downfield by at least 1 ppm and upfield by 2 ppm, respectively, compared to those in a trans conformation. Thus, β- and γ-carbon shifts in proteins seem to be clear markers of proline cis-trans isomerism (Clore et al., 1990), as was established previously for peptides (Howarth and Lilley, 1978).

In general, secondary chemical shifts prove to be sensitive to molecular conformation and environment. Carbon chemical shifts in particular might be more sensitive than ^1H chemical shifts as a probe for secondary structure, since ^{13}C resonances are less affected by electrostatic and ring-current effects, while their dispersion is larger than that of ^1H resonances (Ikura et al., 1991; Wishart et al., 1991). Statistical studies (Spera and Bax, 1991; Wishart et al., 1991) give evidence of a strong dependence of $^{13}C^{\alpha}$ chemical shifts on backbone conformation (ϕ,ψ angles). Residues in α-helix or β-sheet define two distributions of α-carbon shift values, with little overlap between them. Opposite, but less marked tendencies are found for β-carbon resonances. Similar results were obtained from ab initio computations (de Dios et al., 1993; Laws et al., 1993).

Figure 5 displays the ^{13}C secondary chemical shifts of the α- and β-carbons versus the amino acid sequence. Chemical shifts of residues Ala^2, Thr^8, Asp^{48} and Gly^{104} have been corrected, by

TABLE 1
^{13}C CHEMICAL SHIFTS (ppm) OF APO-NEOCARZINOSTATIN

Residue	C^{α}	C^{β}	C^{γ}	C^{δ}	Others	Residue	C^{α}	C^{β}	C^{γ}	C^{δ}	Others
Ala[1]	49.45	17.0				Gly[43]	44.3				
Ala[2]	48.3	15.9				Val[44]	59.95	31.85	17.75, 19.8		
Pro[3]	60.5	30.1	24.85	48.2		Leu[45]	51.0	41.75	23.85	21.5, 20.9	
Thr[4]	58.8	70.6	19.1			Ala[46]	47.75	19.25			
Ala[5]	48.35	19.95				Cys[47]	54.7				
Thr[6]	58.25	69.8	19.0			Asp[48]	48.05	35.65			
Val[7]	59.0	32.85	21.0, 19.9			Pro[49]			24.6	49.9	
Thr[8]	56.45	69.75	18.3			Ala[50]	52.4	16.65			
Pro[9]	62.0	32.15	22.05	47.6		Asp[51]	51.45	40.9			
Ser[10]	55.55	62.45				Phe[52]	54.05				128.95 (C^{δ}); 128.45 (C^{ε}); 126.3 (C^{ζ})
Ser[11]	54.1	63.35									
Gly[12]	44.15					Ser[53]	53.6	63.25			
Leu[13]	52.55	40.2	24.0	20.35, 24.4		Ser[54]	55.2	62.4			
Ser[14]	54.2	63.1				Val[55]	57.2	31.2	18.15, 20.2		
Asp[15]	55.0	39.9				Thr[56]	59.4	67.7	18.85		
Gly[16]	43.65					Ala[57]	50.1	17.6			
Thr[17]	62.75	67.4	20.05			Asp[58]	50.6	38.9			
Val[18]	59.7	29.85	19.05, 19.7			Ala[59]	52.4	16.0			
Val[19]	56.5	33.35	20.3, 18.95			Asn[60]	50.25	37.35			
Lys[20]	53.0	31.15	22.5	26.45	39.65 (C^{ε})	Gly[61]	44.4				
Val[21]	58.5	32.35	?, 18.2			Ser[62]	54.7	63.25			
Ala[22]	48.0	19.55				Ala[63]	49.5	21.25			
Gly[23]	41.6					Ser[64]	55.25	63.15			
Ala[24]	48.75	19.8				Thr[65]	57.75	66.3	16.6		
Gly[25]	44.25					Ser[66]	55.25	63.25			
Leu[26]	50.8		24.1	18.0, 23.35		Leu[67]	51.9	45.25	26.15	22.9, 25.8	
Gln[27]	53.25	26.4	31.8			Thr[68]	60.85	66.6	19.25		
Ala[28]	51.45	17.2				Val[69]	57.7	32.15	16.9, 19.8		
Gly[29]	43.65					Arg[70]	49.5			40.7	
Thr[30]	61.1	67.7	19.1			Arg[71]				41.4	
Ala[31]	49.2	17.0				Ser[72]	53.25	63.45			
Tyr[32]	55.0	39.4			116.95 (C^{ε})	Phe[73]	53.45	38.4			128.15 (C^{δ}); 128.2 (C^{ε}); 126.9 (C^{ζ})
Asp[33]	51.15	38.55									
Val[34]	58.2	30.2				Glu[74]	53.75	26.55			
Gly[35]						Gly[75]	43.7				
Gln[36]	51.1	28.4				Phe[76]	55.05	40.95			
Cys[37]	53.8					Leu[77]	52.05	39.75	25.6	22.85, 20.4	
Ala[38]	49.0	22.4				Phe[78]	58.6	36.4			
Trp[39]	54.1	25.7			125.1 ($C^{\delta 1}$); 118.2 ($C^{\varepsilon 3}$); 119.5 ($C^{\zeta 3}$); 122.4 ($C^{\eta 2}$); 112.6 ($C^{\zeta 2}$)	Asp[79]	50.85	37.5			
						Gly[80]					
						Thr[81]	61.6	67.3	19.85		
						Arg[82]	54.75	28.2	25.1	40.9	
						Trp[83]	57.7	28.3			124.25 ($C^{\delta 1}$); 117.4 ($C^{\varepsilon 3}$); 119.85 ($C^{\zeta 3}$); 122.35 ($C^{\eta 2}$); 112.6 ($C^{\zeta 2}$)
Val[40]	59.15	30.2	20.1, 14.7								
Asp[41]	50.8	40.1									
Thr[42]	62.05	66.3	19.5								

TABLE 1
(continued)

Residue	C^{α}	C^{β}	C^{γ}	C^{δ}	Others	Residue	C^{α}	C^{β}	C^{γ}	C^{δ}	Others
Gly^{84}	41.2					Ala^{100}	52.4	16.45			
Thr^{85}	62.05	66.85	19.6			Ala^{101}	49.25	17.0			
Val^{86}	59.3	30.25	19.1, 19.6			Gly^{102}	43.05				
Asp^{87}	49.8	40.0				Asn^{103}	50.35	37.65			
Cys^{88}						Gly^{104}	43.15				
Thr^{89}	62.55	66.75	19.4			Pro^{105}	59.7	29.7	24.7	46.35	
Thr^{90}	59.9	67.7	19.35			Glu^{106}	55.0	27.2	33.0		
Ala^{91}	48.9	18.05				Gly^{107}	42.5				
Ala^{92}	49.15	15.7				Val^{108}	59.3	31.7	?, 23.85		
Cys^{93}	52.05					Ala^{109}	51.05	17.0			
Gln^{94}	51.8	30.9	29.65			Ile^{110}	56.35	39.4		12.2	15.25 ($C^{\gamma 2}$)
Val^{95}	58.5	31.35	?, 20.45			Ser^{111}	54.6	63.8			
Gly^{96}	42.3					Phe^{112}	54.7	39.15			129.65 (C^{δ}); 128.15
Leu^{97}	52.2	43.1	24.55	23.9, 24.5							(C^{ϵ}); 127.4 (C^{ζ})
Ser^{98}	54.8	63.8				Asn^{113}	52.5	37.5			
Asp^{99}	50.05										

The ^{13}C chemical shifts are indirectly referenced to TMS. For residues valine and leucine, which have two methyl carbons of the same type (γ or δ), the carbon that corresponds to the downfield ^{1}H methyl chemical shift is listed first. Of the protonated carbon resonances of apo-neocarzinostatin, 90% have been assigned (127 out of 130 methine resonances, 20 out of 27 aromatic resonances, 75 out of 92 methylene resonances and 64 out of 69 methyl resonances). Experimental conditions: pH 5.5, 308 K.

addition of 2 and 0.8 ppm to the $^{13}C^{\alpha}$ and $^{13}C^{\beta}$ shifts, respectively, to suppress the contribution of the following proline residue to their shielding. Both C^{α} and C^{β} schemes are well correlated with the localization of β-strands, α-resonances being shifted upfield and β-resonances downfield. However, the latter appear to be less related to the secondary structure, which could be expected from earlier statistical results (Spera and Bax, 1991). We then focus our attention on the α-carbon shifts. To give a more striking picture of the relationship between secondary shifts and secondary structure in protein, Fig. 6 shows smoothed data, obtained using a window of n = 3. This representation was proposed by Pastore and Saudek (1990) to average out local effects responsible for irregular behaviour of secondary chemical shifts versus protein sequence (like ring-current effects of spatially close aromatic side chains or local fields from charged neighbours). In this plot, β-type structural regions clearly correspond to rather large negative values (lower than −1 ppm), while other regions experience shifts closer to random coil values (i.e., closer to zero). Of particular interest are the loops involved in the active site. The β-ribbon formed by residues 37–47 displays negative secondary shifts, characteristic of well-defined β-structure, except in the hairpin region ranging from residues 41 to 43. In contrast, the other β-ribbon composed of residues 72–87 exhibits weak smoothed secondary shifts. The amino acid composition could partially explain this disparity. In fact, residues 72–87 are very likely perturbed by ring-current effects, due to the presence of four aromatic rings: Phe^{73}, Phe^{76}, Phe^{78} and Trp^{83}. However, the discrepancies between these two β-regions may depend mainly upon differing structural mobilities. Flexibility of both ribbons involved in the active site was invoked as being responsible for the great disper-

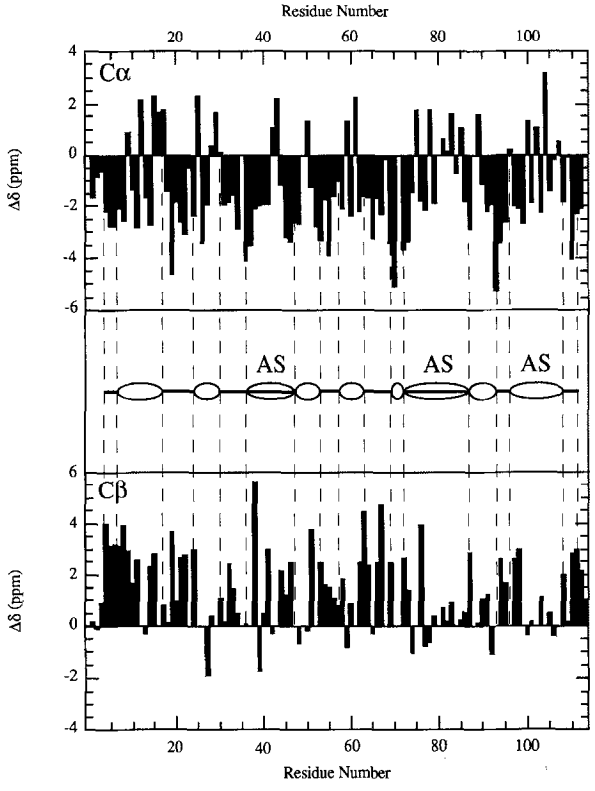

Fig. 5. Secondary shifts of α-carbons (top) and β-carbons (bottom) versus the amino acid sequence, and secondary structure of apo-neocarzinostatin. Random coil values were taken from Wüthrich (1976). Respectively 2 and 0.8 ppm are added to the $^{13}C^{\alpha}$ and $^{13}C^{\beta}$ secondary shifts of residues 2, 8, 48 and 104, to suppress the contributions of the following proline residues. Null values in the plots correspond to nonassigned resonances or, for β-carbons, to glycine residues. The main elements of secondary structure are marked between the two schemes, using continuous thick lines for β-sheets and oval shapes for loops. The locations of the three loops involved in the active site (the two antiparallel β-ribbons involving residues 37 to 47, 72 to 87 and the large loop extending from residues 97 to 107) are indicated by the letters AS.

sions observed both in the rms deviations derived from the NMR data (Adjadj et al., 1992a,b) and in the crystallographic B-factors (Teplyakov et al., 1993). Weak secondary shifts like those experienced by the second ribbon have been correlated with unstructured regions or with high segmental fluctuations of structured regions (Pastore and Saudek, 1990; Wishart et al., 1991). In contrast, the clear negative values found for the first ribbon are indicative of a more structural rigidity of this loop, probably reinforced by the presence of the disulfide bridge between Cys^{37} and Cys^{47}. This suggests that the relatively higher mobility of the region of residues 72–87 is of prime importance for the association with the chromophore. Finally, the weak secondary shifts also observed for the third loop of the active site (residues 97–107) are well correlated with the likely high flexibility of this unstructured region.

CONCLUSIONS

The present work demonstrates the possibility to identify nearly all the resonances of a 10.7-

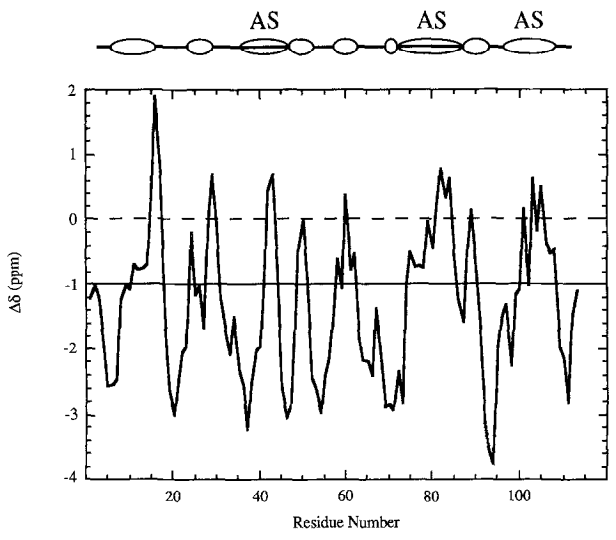

Fig. 6. Smoothed $^{13}C^{\alpha}$ secondary shifts as a function of the residue number and secondary structure for apo-neocarzinostatin. Shift values are identical to those used in Fig. 5. Smoothing was performed by averaging each point with its preceding and following neighbours. Structural elements are indicated as in the previous figure.

kDa protein at natural ^{13}C abundance, provided the ^{1}H spectrum has already been assigned. The basic pulse sequences used in the assignment procedure are HMQC, HMQC-RELAY and HMQC-NOESY. Other experiments, namely double-DEPT and triple-quantum experiments, have been performed in order to selectively observe CH or CH_2 resonances with optimum sensitivity. In particular, the triple-quantum scheme has been adapted from its original form to suppress non-^{13}C-bound protons prior to detection, by means of a z gradient pulse. α-Carbon chemical shifts, unlike β ones, are found to correlate quite well with the secondary structure of apo-neocarzinostatin. In addition, qualitative information on main-chain flexibility may be deduced from smoothed alpha secondary shifts. The present data will allow interpretation of carbon relaxation time measurements, providing an insight into internal motions of apo-neocarzinostatin. These motions are of particular interest, since they might be implicated in the biological activity of this carrier protein. This analysis is currently in progress in our laboratory.

ACKNOWLEDGEMENTS

We thank Dr. V. Favaudon for providing a sample of purified apo-neocarzinostatin. Financial support from Ligue Nationale Contre le Cancer, Institut Curie and INSERM allowed the completion of this work.

REFERENCES

Adjadj, E., Mispelter, J., Quiniou, E., Dimicoli, J.L., Favaudon, V. and Lhoste, J.M. (1990) *Eur. J. Biochem.*, **190**, 263–271.

Adjadj, E., Quiniou, E., Mispelter, J., Favaudon, V. and Lhoste, J.M. (1992a) *Eur. J. Biochem.*, **203**, 505–511.

Adjadj, E., Quiniou, E., Mispelter, J., Favaudon, V. and Lhoste, J.M. (1992b) *Biochimie*, **74**, 853–858.

Bax, A., Griffey, R.H. and Hawkins, B.L. (1983) *J. Magn. Reson.*, **55**, 301–315.

Bax, A., Ikura, M., Kay, L.E., Torchia, D.A. and Tschudin, R. (1990) *J. Magn. Reson.*, **86**, 304–318.
Bendall, M.R., Pegg, D.T. and Doddrell, D.M. (1983) *J. Magn. Reson.*, **52**, 81–117.
Bodenhausen, G. and Ruben, D.J. (1980) *Chem. Phys. Lett.*, **69**, 185–189.
Brühwiler, D. and Wagner, G. (1986) *J. Magn. Reson.*, **69**, 546–551.
Clore, G.M., Bax, A., Driscoll, P.C., Wingfield, P.T. and Gronenborn, A.M. (1990) *Biochemistry*, **29**, 8172–8184.
Davis, D.G. (1990) *J. Magn. Reson.*, **90**, 589–596.
Davis, D.G. (1991) *J. Magn. Reson.*, **91**, 665–672.
de Dios, A.C., Pearson, J.G. and Oldfield, E. (1993) *Science*, **260**, 1491–1496.
Doddrell, D.M., Pegg, D.T. and Bendall, M.R. (1982) *J. Magn. Reson.*, **48**, 323–327.
Domke, T. and Leibfritz, D. (1990) *J. Magn. Reson.*, **88**, 401–405.
Ernst, R.R., Bodenhausen, G. and Wokaun, A. (1987) In *International Series of Monographs on Chemistry*, Vol. 14 (Eds, Breslow, R., Halpern, J. and Rowlinson, J.S.) Clarendon Press, Oxford, pp. 467–489.
Gao, X. and Burkhart, W. (1991) *Biochemistry*, **30**, 7730–7739.
Gao, X. (1992) *J. Mol. Biol.*, **225**, 125–135.
Howarth, O.W. and Lilley, D.M.J. (1978) *Prog. NMR Spectrosc.*, **12**, 1–40.
Ikura, M., Spera, S., Barbato, G., Kay, L.E., Krinks, M. and Bax, A. (1991) *Biochemistry*, **30**, 9216–9228.
Kappen, L.S., Napier, M.A. and Goldberg, I.H. (1980) *Proc. Natl. Acad. Sci. USA*, **77**, 1970 1974.
Kay, L.E., Jue, T.L., Bangerter, B. and Demou, P.C. (1987) *J. Magn. Reson.*, **73**, 558–564.
Kay, L.E. and Bax, A. (1989) *J. Magn. Reson.*, **84**, 598–603.
Kessler, H., Schmieder, P. and Kurz, M. (1989) *J. Magn. Reson.*, **85**, 400–405.
Kim, K.H., Kwon, B.M., Myers, A.G. and Rees, D.C. (1993) *Science*, **262**, 1042–1046.
Laws, D.D., de Dios, A.C. and Oldfield, E. (1993) *J. Biomol. NMR*, **3**, 607–612.
Lerner, L. and Bax, A. (1986) *J. Magn. Reson.*, **69**, 375–380.
London, R.E. and Avitabile, J. (1978) *J. Am. Chem. Soc.*, **100**, 7159–7165.
Müller, L. (1979) *J. Am. Chem. Soc.*, **101**, 4481–4484.
Nirmala, N.R. and Wagner, G. (1988) *J. Am. Chem. Soc.*, **110**, 7557–7558.
Norton, R.S., Clouse, A.O., Addleman, R. and Allerhand, A. (1977) *J. Am. Chem. Soc.*, **99**, 79–83.
Norwood, T.J., Boyd, J., Heritage, J.E., Soffe, N. and Campbell, I.D. (1990) *J. Magn. Reson.*, **87**, 488–501.
Oh, B.H., Westler, W.M. and Markley, J.L. (1989) *J. Am. Chem. Soc.*, **111**, 3083–3085.
Oldfield, E., Norton, R.S. and Allerhand, A. (1975) *J. Biol. Chem.*, **250**, 6368–6380.
Palmer III, A.G., Cavanagh, J., Wright, P.E. and Rance, M. (1991) *J. Magn. Reson.*, **93**, 151–170.
Pastore, A. and Saudek, V. (1990) *J. Magn. Reson.*, **90**, 165–176.
Remerowski, M.L., Glaser, S.J., Sieker, L.C., Samy, T.S.A. and Drobny, G.P. (1990) *Biochemistry*, **29**, 8401–8409.
Ribeiro, A.A., King, R., Restivo, C. and Jardetzky, O. (1980) *J. Am. Chem. Soc.*, **102**, 4040–4051.
Richarz, R., Nagayama, K. and Wüthrich, K. (1980) *Biochemistry*, **19**, 5189–5196.
Schmidt, J.M. and Rüterjans, H. (1990) *J. Am. Chem. Soc.*, **112**, 1279–1280.
Shaka, A.J., Keeler, J., Frenkiel, T. and Freeman, R. (1983) *J. Magn. Reson.*, **52**, 335–338.
Shon, K. and Opella, S.J. (1989) *J. Magn. Reson.*, **82**, 193–197.
Sklenar, V., Torchia, D. and Bax, A. (1987) *J. Magn. Reson.*, **73**, 375–379.
Sørensen, O.W., Eich, G.W., Levitt, M.H., Bodenhausen, G. and Ernst, R.R. (1983) *Prog. NMR Spectrosc.*, **16**, 163–192.
Spera, S. and Bax, A. (1991) *J. Am. Chem. Soc.*, **113**, 5490–5492.
Summers, M.F., Marzilli, L.G. and Bax, A. (1986) *J. Am. Chem. Soc.*, **108**, 4285–4294.
Tate, S.I., Masui, Y. and Inagaki, F. (1991) *J. Magn. Reson.*, **94**, 625–630.
Teplyakov, A., Obmolova, G., Wilson, K. and Kuromizu, K. (1993) *Eur. J. Biochem.*, **213**, 737–741.
Wagner, G. and Brühwiler, D. (1986) *Biochemistry*, **25**, 5839–5843.
Wagner, G. (1989) *Methods Enzymol.*, **176**, 93–113.
Wishart, D.S., Sykes, B.D. and Richards, F.M. (1991) *J. Mol. Biol.*, **222**, 311–333.
Wüthrich, K. (1976) *NMR in Biological Research: Peptides and Proteins*, Elsevier, New York, NY, pp. 157–209 and 293–316.
Zhang, X. and Wang, C. (1991) *J. Magn. Reson.*, **91**, 618–623.
Zuiderweg, E.R.P. (1990) *J. Magn. Reson.*, **86**, 346–357.